Display of Clouds Taking into Account Multiple Anisotropic Scattering and Sky Light

Tomoyuki Nishita
Fukuyama University
Sanzo, Higashimura-cho, Fukuyama,
729-02 Japan
nis@eml.hiroshima-u.ac.jp

Yoshinori Dobashi
Hiroshima University
1-4-1, kagamiyama, Higashi-hiroshima,
739 Japan
doba@eml.hiroshima-u.ac.jp

Eihachiro Nakamae
Hiroshima Prefectural University
Nanatsuka-cho, Shoubara City,
727 Japan
naka@bus.hiroshima-pu.ac.jp

Abstract

Methods to display realistic clouds are proposed. To display realistic images, a precise shading model is required: two components should be considered. One is multiple scattering due to particles in clouds, and the other factor to be considered is sky light. For the former, the calculation of cloud intensities has been assumed to be complex due to strong forward scattering. However, this paper proposes an efficient calculation method using these scattering characteristics in a positive way. The latter is a very significant factor when sky light is rather stronger than direct sunlight, such as at sunset/sunrise, even though sky light has been ignored in previous methods.

This paper describes an efficient calculation method for light scattering due to clouds taking into account both multiple scattering and sky light, and the modeling of clouds.

CR Categories and Subject Descriptors:
I.3.3 [**Computer Graphics**]: Picture/Image Generation
I.3.7 [**Computer Graphics**]: Three-Dimensional Graphics and Realism
Key Words: Clouds, Multiple scattering, Sky light, Participating Media, Optical Length, Photo-realism, Radiative Transfer

1 INTRODUCTION

Display of natural scenes such as mountains, trees, the earth, the sea, and the waves have been attempted. This paper discusses the display of clouds. The display of clouds is indispensable for the background images of buildings and flight simulators. For displaying clouds, mapping of fractal textures onto ellipsoids is often used. However, we discuss a display method taking account of light scattering due to cloud particles illuminated by sky light. The color of clouds varies according to the relationship between the viewing direction and the position of the sun. The intensity of clouds is dependent on absorption/scattering effects due to clouds particles.

The albedos of clouds are very high: It is well known that for objects with such a high albedo multiple scattering can not be ignored[4]. Clouds are illuminated by both direct sunlight and sky light affected by atmospheric scattering. Their reflected light from the ground (or the sea) also can not be ignored, and we take these effects into account. That is, this paper discusses not only a local illumination model of clouds, but also a global illumination model taking into account the color variation of incident light on them passing through the atmosphere and sky light.

A brief description of our proposed method is as follows. Clouds are defined by density fields, which are modeled by the metaball technique. Shapes of clouds are modeled by applying the fractal technique to metaballs. The particles they consist of have strong forward scattering characteristics. This was considered as one of the difficulties due to the intensity calculation in the previous work. We use this characteristic in a positive way. That is, the space, which should be calculated, is restricted because the scattering direction is very narrow. For the calculation of multiple scattering, the space containing the clouds is subdivided into a number of volume elements (voxels). As a preprocess, a sample space is prepared, which is defined as a parallelepiped consisting of a set of some voxels with the average density of the clouds, the high order of scattering at a specified voxel from the other voxels in the space is calculated and stored, before the calculation of scattering due to every voxel in the total space. By using this pattern which is the contribution ratio at each voxel in the sample space to the specified voxel, the calculation cost for the total space can be reduced. At least the 3rd order of scattering is calculated in our paper. The spectrum and spatial distribution of sky light are precalculated by taking into account Rayleigh scattering and Mie scattering by assuming negligible attenuation due to cloud particles. The intensity of the first order of scattering at each voxel due to sky light (including reflected light from the ground) can be easily calculated by using the optical depths from the cloud surface, stored in a look-up table.

Finally, several examples are demonstrated in order to show the effectiveness of the method proposed here.

2 Previous Work

Density volume display methods such as those of clouds in previous work are divided into two categories, mapping technique and physical model taking into account scattering/absorption due to particles. For the former, Gardner[7] used a mapping technique of fractal textures onto ellipsoids. For the latter, the displaying of the atmosphere(sky color), water color, and particles such as ice has been developed: a) for light scattering from particles in the air, the shafts of light caused by spot lights[18][9], light beams passing through gaps in clouds or through leaves[15], the sky color taking account of atmospheric scattering[14][12], scattered light due to nonuniform density particles such as clouds and smoke[18][24][10][26], the color of the atmosphere viewed from space[20], the effect of the radiosity of a participating medium[23], and multiple anisotropic volume scattering[16][10][1]. b) the display of the color of water affected by particles in the water, such as ponds[11], the color of the sea as viewed from outer space[20] and optical effects such as shafts of light within water[22]. and c) the display of Saturn's rings (reflective ice particles)[2], and subsurface scattering such as skin[8].

In this paper we focus our discussion on multiple scattering. For high albedo particles, multiple scattering should be calculated. On this, Kajiya[10] was first to offer a solution. For multiple scattering the two-pass method[10][16][23] is usually used. The first pass deposits flux from the light source and the light scattered at each cloud
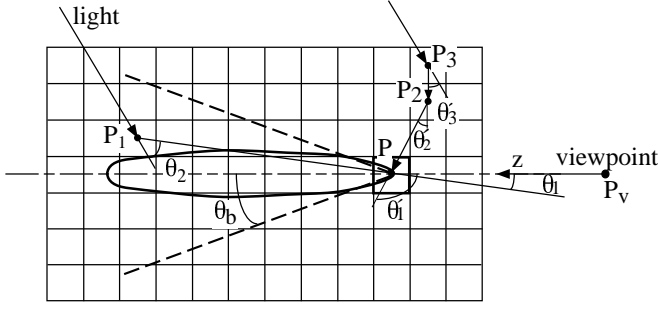
Figure 1: Light paths through clouds.

voxel. The second pass gathers the scattered light along each viewing ray. Kajiya used spherical harmonics to express the intensity distribution of scattered light at each voxel as a function of direction. As cloud particles have strong forward scattering characteristics (caused by a narrow phase function), a relatively high order of spherical harmonics are required for representation of the distribution of light scattered. In the case of the phase function described in section 3.3, the 20th order of harmonics and more than 400 coefficients at each voxel may be required. Max's approach[16] is to allocate the radiosity leaving each volume element into a collection of M direction bins of constant intensity. This discrete ordinate method also requires many direction bins to express such a narrow scattering beam. Even though the distribution of scattering becomes slightly isotropic after multiple scattering, some error appears in the first order of scattering. Blasi[1] used the Monte Carlo method for determining the scattering direction of photons, but he did not calculate the scattered component in the viewing ray. Therefore, this method can not be considered as one which takes into account anisotropic phase function. Hanrahan[8] proposed a method for subsurface scattering, but this method is limited to layered surfaces such as skin and leaves; this method is not applicable to complex shapes such as clouds. Stam [26] took into account multiple scattering to display gaseous phenomena such as fire. He employed LU-decomposition to solve a matrix equation. He ignored the phase function.

Here, we propose a method which takes into account multiple scattering, sky light effects, and reflection from the ground.

3 Shading Model for Clouds

3.1 Basic Ideas

In order to render the particles in clouds, the following elements should be taken into account: (i) Phase functions should be taken into account; scattering by small particles such as air molecules is called Rayleigh scattering, and scattering by aerosols such as dust is called Mie scattering. The sizes of particles in clouds are relatively large (i.e., 2-40 μm), so the particles have strong forward scattering. (ii) The multiple scattering of light among particles in clouds can not be neglected because their albedos are very high[4][25]: 0.7 - 0.9 for cumulus and stratus. (iii) The clouds are illuminated by both direct sunlight and sky light. And they are also illuminated by the reflected light of direct sunlight and sky light from the ground (i.e., reflected groundlight). (iv) The effects of the atmosphere should be considered. The scattered light at the clouds is attenuated by particles in the atmosphere and reaches the viewpoint. Sunlight is absorbed when light passes through the atmosphere. (v) The density distributions of clouds are not uniform.

As shown in Fig.1, the following optical paths or optical effects also should be considered. (1) Particle P in a cloud is illuminated by direct sunlight (I_{sun}), scattered light from the other particles (path

Figure 2: Block diagram for the intensity reaching the viewpoint passing through clouds.

$P_1 P_2 P$), sky light (or sky radiance), and reflected light from the earth. (2) The light reaching viewpoint is determined by every particle on the viewing ray; the incident light of sky light to the cloud at P_b (I_s), particles in clouds ($P_b P_a$), and particles in the atmosphere ($P_a P_v$). The intensity is obtained by integrating all the scattered light due to these particles. The attenuation of light due to these particles is also considered. (3) The sky light consists of light scattered by particles in the air. The spatial and spectrum distribution of sky light depends on the sun position. The atmosphere consists of air molecules and aerosols; their scattering characteristics obey Rayleigh scattering and Mie scattering, respectively. The density distributions of air molecules and aerosols vary exponentially with altitude. (4) The reflected light from the earth consists of the direct sunlight and sky light. The direct sunlight is attenuated by the path $P_s P_e$ and the reflected light is also attenuated by the path $P_e P$. The scattered light due to particles on these paths are added.

As described above, the optical paths are complicated, we can express these optical effects as the block diagram, as shown in Fig.2.

This paper discusses a rendering algorithm for clouds taking into account at least the 3rd order of multiple scattering.

3.2 Calculation of Light Scattering for Clouds

Let's discuss first the calculation method for single scattering due to cloud particles.

As shown in Fig.1, let's denote the intensity of incident sunlight to a cloud as I_c and the intensity of that behind the cloud (i.e., sky light) as I_s, the intensity of light from the cloud at P_a, I_a, which is the summation of the attenuated light of scattering on $P_a P_b$ of the viewing ray and the attenuated sky light I_s due to the cloud. I_a can be obtained by the following equation:

$$
\begin{aligned}
I_a(\lambda) &= I_s(\lambda)exp(-\tau(P_a P_b, \lambda)) \\
&+ \int_{P_a}^{P_b} I_p(\lambda)\beta\rho(l)F(\theta)exp(-\tau(PP_a, \lambda))dl, \quad (1)
\end{aligned}
$$

where the first term means the incident light at P_b is attenuated by particles on the path of $P_a P_b$, and the second the scattered light due to particles on the path. λ is the wavelength of the light, F the scattering phase function indicating the directional characteristics of scattering, θ the scattering angle (see Fig. 1), ρ the density, I_s the intensity of the sky light in the viewing direction, τ the optical length obtained by integrating the attenuation coefficient β along the path, i.e., given by $\tau(S, \lambda) = \int_0^S \beta\rho(s)ds$ (S is path length).

As the incident light at point P has been attenuated due to movement through the cloud ($P_c P$), the incident intensity at P is obtained by,

$$
I_p(\lambda) = I_c(\lambda)exp(-\tau(PP_c, \lambda)), \quad (2)
$$

where I_c is the attenuated light of I_{sun} which is the solar radiation at the top of the atmosphere. Equation (1) is rewritten by using gains

Figure 3: Calculation of multiple scattering and reference pattern.

G_a and G_s;

$$I_a(\lambda) = I_s(\lambda)G_a(\lambda) + I_c(\lambda)G_s(\lambda). \quad (3)$$

Therefore, the intensity reaching the viewpoint is represented by the block diagram as shown in Fig. 2. As shown in Figs. 1 and 2, the types of the incident light onto the cloud are the intensity of sky light in the viewing direction, I_s, the attenuated intensity of I_{sun}, sky light I_{sky}, and the reflected light from the ground. See reference [20] for the calculation method for atmospheric scattering. The light reaching viewpoint P_v can be obtained as the remainder after scattering and absorption due to air molecules along the path between P_a and P_v. The calculation methods for multiple scattering and sky light (including reflection from the ground) are described in section 3.4 and 3.5, respectively.

3.3 Phase Function

Scattering of light due to particles (water droplets) in clouds obeys Mie scattering. The characteristics of scattering depend on the size of the particles, and have strong forward scattering. That is, when the scattering angle θ (see Fig. 1) is greater than $10°$, the scattering intensity becomes less than 10%, compared to that at angle $0°$. As various sizes of particles exist, the phase function is expressed by the linear combination of several phase functions;

$$F(\theta) = \sum_{i=0}^{K} w_i F_i(\theta), \quad (4)$$

where K is the number of types of functions, and w_i is weight for phase function i. The Henyey-Greenstein function is well known as a phase function. Recently, Cornette[6] improved it, which gives more reasonable physical expression:

$$F(\theta, g) = \frac{3(1 - g^2)}{2(2 + g^2)} \frac{(1 + cos^2\theta)}{(1 + g^2 - 2gcos\theta)^{3/2}}, \quad (5)$$

where g is an asymmetry factor and is a function (see [20]) which is determined by the cloud condition and the wave length (see references[6] for the parameters of clouds). If $g = 0$, this function is equivalent to Rayleigh scattering. In this paper, two functions, Rayleigh (e.g., 5%) and Mie scattering (the remainder) for cloud particles, are combined.

For scattering due to clouds the spectrum of scattering is not much influenced compared with scattering due to air molecules. Therefore, the color of clouds depends on the spectrum of incident light.

3.4 Multiple Scattering

For solving multiple scattering phenomena, two methods have been developed; solving integral equations and using the Monte Calro

method. This paper combines both of these. The space including some clouds is subdivided into a number of volume elements, and shooting/receiving energy among them is calculated. For calculating its exchanging energy among the elements, a form factor generally used in radiosity methods is useful. Rushmeier[23] introduced the volume/volume form factor: form factor F_{kj} represents the ratio of the total scattered and emitted energy leaving element V_k which is absorbed or scattered by volume element V_j, but her method is limited to isotropic scattering. The phase function is an important factor for energy transport. In our method the form factors are calculated by taking into account the phase function. That is, in the numerical integral for form factors the phase functions having angles between the viewpoint and sub-voxels are multiplied. Let's consider the beam spread which is an angle including most of scattered energy (see θ_b in Fig. 3). Every volume element within the beam spread of the phase function is subdivided into smaller sub-voxels compared with the regular voxels.

Let's denote the intensity at point P in direction ω as $I(P, \omega)$, the extinction coefficient per unit length as β, the length of cloud in viewing ray S, the path length from P as s ($s = 0$ at P, P_S ; S from P). Then $I(P, \omega)$ is expressed by

$$I(P, \omega) = I(P_S, \omega)exp(-\tau(PP_S))+$$
$$\int_{s=0}^{S}[\beta\rho(s)exp(-\tau(P(s)P))\frac{1}{4\pi}\int_{4\pi}F(\theta)I(P, \omega')d\omega']ds, \quad (6)$$

where θ is phase angle between ω and ω': ω' is angular variable for integration. The problem is that I exists in both sides of the equation. To solve this, this space is subdivided into a number of volume elements. If we denote the number of voxels as N, and the number of the discrete directions as M, then MN matrix equations should be solved.

For a narrow phase function (strong forward scattering), the matrix becomes sparse because even if some volume elements existing outside of the beam spread shoot their energy to the volume element P to be calculated, the energy hardly contribute to the intensity at P in the viewing direction. The form factors for distant pairs of elements are very small. Therefore, we can predict which voxel affects a specified volume element. That is, a sample space is prepared, light scattering in the space is calculated before the calculation of scattering due to every voxel in the whole space. By using the contribution pattern of voxels in the sample space, the calculation cost can be reduced. Fig.3 shows a sample space, the ellipsoid means the scaled phase function when the viewpoint is assumed as a light source. This region tells us which voxels contribute to scattering at point P. The contribution ratio of voxel at P_1 to P is high because it exists within the beam spread.

For a given viewpoint and a light direction, assume the uniform density (average density), and then calculate the voxels which affect a specified voxel. The scattered light in the viewing direction at point P through every path of the 2nd and 3rd orders of scattering are calculated (e.g., P_1P; 2nd order path,P_3P_2P; 3rd order path in Fig.3). These results, the 2nd and 3rd order components, are stored at each voxel and the total scattered intensity at P due to every voxel is calculated. By using these results, each contribution ratio to the total intensity can be obtained. We refer to this contribution-ratio pattern in a look-up table as a *reference pattern (or a template)*. For simplifying, the z-axis of the voxel is assumed to be in line with the viewing ray. That is, the edges of the voxel coincide with the principal axes of the eye coordinates system.

For N voxels, the number of paths for the 2nd order of scattering is $(N - 1)$, and the number of paths for the 3rd order of scattering is $(N - 1)^2$. In our experiments, when $8 \times 8 \times 16$ voxels are used as a reference pattern, 1,046,529 paths were required for the 3rd order of the scattering, but only 400 paths effectively contribute 90% of the

total intensity. The above size of voxels is just an example, we used more large sizes of the reference patterns as described later. For the 3rd order of scattering, it is equivalent to that the intensity is determined by multiplying two form factors and three phase functions of angles of θ'_1, θ'_2 and θ'_3, as shown in Fig.3.

In our examples, the percentages of the 2nd and 3rd order of scattering are roughly 10-40% and 1-3% for small phase angles (less than $10°$), 40-70% and 2-10% for large phase angles: these data depend on the conditions such as cloud density. For the large phase angles, the higher order of scattering may be required. But to save the computation time, we truncated more than 4th order of scattering.

In general, as geometric factors, such as form factors and phase angles, are much more effective compared with the density distribution, we assumed that the contribution pattern of voxels taking into account non-uniform density is close to the reference pattern of uniform density. The voxels in the whole space are scanned by the reference pattern; this process is similar to filtering in image processing, in our case the reference pattern being equivalent to a 3-D filter.

The proposed algorithm includes the following steps:

step 1) : The center of the reference pattern is set to voxel P to be calculated, and the intensities of light scattered due to other voxels affecting voxel P are calculated and are accumulated on the strength of the reference pattern; the voxels whose contribution ratios are higher than a given threshold are selected. The form factors between each pair of voxels are stored over the look-up table along with the reference pattern. In our method, the modified form factors are stored as described before: they are obtained by multiplying the values of phase functions.

step 2) : The attenuation ratio (or optical length) for the sunlight at each voxel is stored. Moving the reference pattern, voxel by voxel, over the whole space, the light scattered (the 2nd and 3rd order of scattering) in the viewing direction at each voxel can be stored. The density distribution of the sample space for the reference pattern and the whole space to be calculated are different. So, the attenuation between the voxels should be calculated, even though the stored data in the reference pattern for the form factors and the values of phase functions can be used.

step 3) : For each pixel, the intensity is obtained by line integral: the intensity of the 1st order of scattering at a sampling point on the viewing ray is calculated by using the attenuation ratio stored at each voxel, and the intensities of the 2nd and 3rd order of scattering at the sampling point are interpolated from them stored at voxles.

As examples, Fig.4 shows the distribution of voxels with high contribution ratios in the cases of the phase angle of $10°$ and $160°$, respectively. In the figure, the viewpoint is located on the left side, the black lines show the paths having a high contribution to the 2nd order of scattering (i.e., scattered twice like path P_1P in Fig.3), the green lines show the 1st path with a high contribution to the 3rd order of scattering (i.e., scattered three times), and the pink lines show the 2nd path with the maximum contribution to the voxels with a high contribution to the 3rd order of scattering. Let's consider the 2nd order scattering. As shown in Fig.5, the distribution of voxels which have high contribution ratios (e.g., more than 80%) are categorized into the following two cases.
Case A): light source and viewpoint are located in the opposite sides (Fig.5(a)).
Case B): light source and viewpoint are located in the same side (Fig.5(b)).
In both of these cases, three sub-spaces, R_f, R_b, and R_c, contribute to the light scattered at voxel P in the viewing direction. The 1st order of scattering due to particles in R_f is strong because of the small phase angle, even though the 2nd order of scattering at P is weak because of the large phase angle. Even though the 1st order of scattering in R_b is weak because of a large phase angle, the 2nd
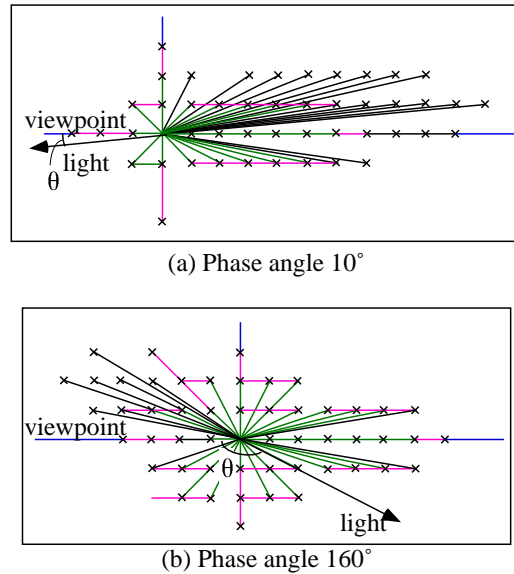

(a) Phase angle 10˚

(b) Phase angle 160˚

Figure 4: Examples of reference patterns.

order of scattering at P is strong because of the small phase angle. In R_c distances of voxels from P are very close, so the form factors are large even though the phase functions are small. As shown in these figures, the sub-spaces with high contribution ratios depend on the light and viewing directions, and they also depend on the size of voxel, density, and extinction coefficients. Thus the size of the reference pattern is adaptively determined. First, we prepare a large sample space (e.g., $30 \times 30 \times 30$ voxels). And we can get the reasonable size of the reference pattern by the following method. To get the reference pattern, every possible path in a sample space is examined, and the bounding box of voxels having high ratios is selected as the reference pattern.

Even though the computational cost is reduced by this method, it is not sufficient. Therefore, we employ the following additional stochastic method. The voxels to be calculated are selected by using random numbers within the paths with a high contribution ratio. The summed intensity of these paths is corrected by using the ratio of the selected paths: assuming the number of the calculated paths to be n_1, the number of paths with a high contribution rate to be n_2, the summed intensity as I, and the total contribution ratio due to n_2 paths as r, then the intensity can be estimated by Irn_2/n_1. In our experiments, only 10% of the voxels in the reference pattern contribute 50% of the total intensity in a case. To use these voxels with high possibility we can improve the accuracy. We uses the constant density assumption for the sample space. If the sub-space to be calculated has wide range of density, it is solved by increasing ratio r. We set $r = 0.8$ in our examples. In the preprocessing stage (i.e., step 1: obtaining the reference pattern), the paths, whose contribution ratio are higher than r, are selected. Though we have discussed multiple scattering up to the 3rd order, the idea using the reference pattern can be expanded to higher orders.

Applying the method described above, the intensity at each voxel can be obtained and be stored. In the rendering step, the intensities at each sampling point on the viewing ray are integrated. In order to obtain high accuracy, the intensity of the first order scattering is calculated at each sampling point even though tri-linear interpolation is used for the intensity of the higher order of scattering and the attenuation (or optical depths) stored at each voxel.

3.5 Atmospheric Effects (Sky Light)

Clouds are visible even if the sun is hidden behind other clouds, after sunset or before sunrise; in other words, the intensity of the sun-
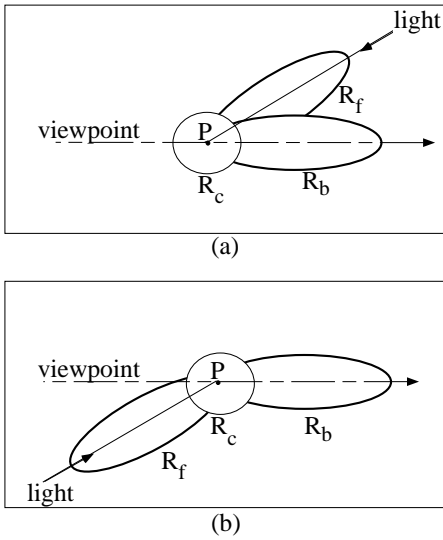
Figure 5: Sub-spaces with high contribution ratios.

light is rather feeble. This implies that sky light can not be ignored.

The intensity of sky light is determined by the scattering and/or absorption of air molecules and aerosols. The former obeys Rayleigh scattering (proportional to the fourth power of the wave length) while the latter obeys Mie scattering. The color of sky light changes depending on the altitude of the sun and the observer's position. Note that the intensity of the sky around the sun is stronger than elsewhere. See reference[20] for the calculation method for sky light. Direct sunlight attenuates when passing through the atmosphere. The incident light to a cloud (see Figs. 1 and 2), I_s, is attenuated sunlight and the light scattered due to particles in the atmosphere.

In meteorology it is well known that the brightness of clouds is affected by the reflected light from the ground. The reflected light from the ground is assumed as upward sky light because of the scattered light due to particles between the cloud and the ground. The reflected light has two components; direct sunlight and sky light. See reference[20] for the calculation method for the reflected light from sky light. Even though the albedo of the ground depends on materials such as soil, trees, sand, we used average albedos (spectrum reflectivity in this case) used in reference[25] which are weighted averages of that of each material.

Single scattering for sky light (and reflected light from ground) is calculated as follows. Ignoring attenuation by cloud particles, a particle (i.e., voxel) is illuminated by the sky light from every direction: The light scattered in the viewing direction arrives at the viewpoint. Since the sky dome can be considered a hemisphere with a large radius[17], the particle can be considered at the center of the hemisphere. Thus, it is possible to take it for granted that the radiance distribution incident onto each particle in a cloud is identical (assuming the difference in the altitude is small). In the case of the calculation of sky light on the ground, the hemisphere is enough. But clouds exist at a high altitude, so the sky light from the bottom should also be considered: the top hemisphere is due to pure sky light and the bottom hemisphere consists of the light scattered due to particles in the bottom of clouds and the attenuated light of reflected light from the ground. The sky dome is divided into several sky elements, and the intensity of the light scattered in the view direction I_v is obtained by calculating the solid angle of the sky elements and their intensities.

In practice, the incident light onto a particle is attenuated by the other particles in the cloud. Therefore, the attenuation factor (transmittance) toward each sky element which is caused by them and which is obtained from its optical length, should be taken into ac-
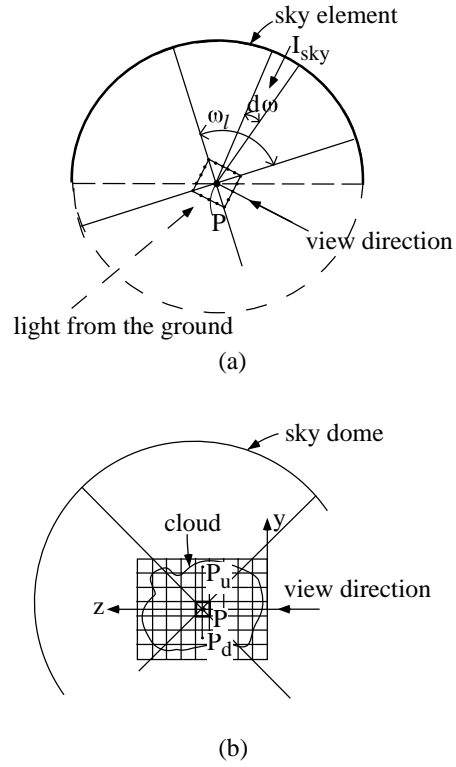

Figure 6: Calculation of skylight.

count. Let's denote the number of the sky elements as K, I_v is obtained by

$$I_v(\lambda) = \sum_{l=0}^{K} t_l \int_{\omega_l} F(\theta) I_{sky}(\omega, \lambda) d\omega = \sum_{l=0}^{K} t_l I_l(\lambda), \quad (7)$$

where t_l is the attenuation factor for the direction of sky element l due to cloud particles, w_l is a solid angle of sky element l, F the phase function, and I_{sky} is the intensity of sky element l, and I_l is the integrated intensity for the sky element. In the rendering process, the attenuation factors t_l from each particle on the viewing ray to all sky elements must be calculated. To calculate these efficiently, we use a look-up table. We make use of the fact that it is easy to calculate the optical length in both the principal and diagonal axes of the voxel.

Let's consider the six faces comprising of the voxel as a simple example (see Fig. 6(a)). The incident light of sky light passing through each face can be calculated by setting the eye at the center of the cube. Each face of the cube is divided into small meshes, which is similar to the hemi-cube method[5]. The attenuation factors (or optical depths) in x, y, and z-directions can be used for six sky elements. Thus, if the accumulated attenuations for each axis are calculated once and stored at each voxel, it is sufficient to get the intensity at the viewpoint by multiplying the attenuation coefficient t_l by the intensity at the voxel and make a summation of them. Note that, in the case of the first order scattering, the intensity of the sky in the viewing direction is the most important as the forward scattering is strong. For example, let's consider the attenuation in y direction at voxel P (see Fig. 6(b)). At voxel P, the attenuation, t, between P and P_u was stored. If the attenuation at P_d is t_d, the attenuation between P_d and P is easily calculated as t/t_d. Even though we only describe for six directions, it is possible to increase the accuracy by preparing the attenuations in other directions, such as diagonal. As described above, sky elements around the sun are very significant since the intensity surrounding the sun is much greater.

To take this into account, the attenuation in the sun's direction stored at each voxel can be utilized.

In addition to the density, the attenuation in the sun's direction, the attenuation factors in $K/2$ directions, and the intensity of light due to the higher order scattering are stored for each voxel.

4 MODELING OF CLOUDS

For modeling clouds, controlling its shape and density distribution is necessary. In this paper, the density distribution of the cloud is defined by using the meta-ball technique[21] (or blobs[3]). Each meta-ball is defined by its center, radius, and the density at the center of the ball. The field value at any point is defined by distances from the specified points in space. The density distribution of a meta-ball is given by a polynomial function in degree 6 of the distance from its center([21]). The surface of a cloud is defined by the isosurfaces of potential fields defined by the meta-balls.

In the rendering process, the intersection of the isosurface (i.e., cloud surface) with a viewing ray is calculated by ray tracing, which effectively expresses the density distribution on a ray by using Bézier function of degree 6 (see [21]). Bézier Clipping[19] is employed for the calculation of intersections.

First, several meta-balls are arranged to form the basic shape of the cloud. Then, small meta-balls on the surface of the cloud are generated recursively by using the following fractal method to form the subtle fringe of the cloud.

The method of generating new balls on a curved surface is as follows. The isosurface is extracted by the marching-cubes algorithm [13] and triangulated. New balls are then generated within each triangle (their positions and radii are determined randomly). Generating new balls produces a new surface, which is again triangulated. And again new balls are generated. This procedure is repeated. By making the radius smaller the further from the center of the cloud, the smaller balls appear around the fringe.

The bottom of a cloud is sometimes relatively flat, and the top of it is bumpy. To realize this kind of shape, the normal vectors of the generated triangles on the iso-surface can be used. If the normal vector is not downward new balls are created, otherwise the generation of balls is limited. By using this technique we can control the cloud shape, and make possible clouds which grow upwards.

5 EXAMPLES

Fig. 7 shows an example of clouds: the altitude of the sun in Figs.(a), (b), and (c) is $65°$, $10°$ and $5°$ (sunset), respectively. These examples depict beautiful variations in the color of the clouds and sky. One can see the bright edges of cloud in Fig.(b) because the sun is behind the cloud.

Fig.8 shows examples of cumulonimbus. The atmospheric effect between the clouds and the viewpoint is calculated, so the color of the clouds is bluish (Fig.(a)) or reddish (Fig.(b)). The number of meta-balls for these clouds for Figs.7 and 8 are 338 and 358, respectively.

This calculation was done on an IRIS Indigo2 (R4400). The computation times for Fig.7 (a), and Fig.8 (a) were 20 minutes, and 31.3 minutes, respectively (image width=500).

In these examples, the size of voxels is 100^3 in average, but if they are sparse, we could save the memory by using the list-structure.

6 CONCLUSION

We have proposed an algorithm for a physical based image synthesis of clouds. As shown in the examples, the proposed method gives us photo-realistic images taking into account anisotropic multiple scattering and sky light. The advantages of the proposed method are as follows:

(1) For anisotropic multiple scattering, the optical paths of the light scattered in the viewing direction are limited because of strong forward scattering (a narrow phase function). Employing the pattern expressing the contribution ratio at each voxel to the specified voxel in the sample space, the calculation cost for the total space can be reduced.

(2) For sky light, the spectrum of the sky light is calculated by taking into account scattering/absorption due to particles in the atmosphere, and the intensity of light scattered at one voxel illuminated by each sky element is stored. The intensity of the first order scattering at every voxel due to sky light can be easily calculated by using the optical depths from the cloud surface stored in a look-up table. The reflected light from the ground can be calculated by treating it as upward sky light.

(3) The clouds can be modeled by using metaballs. The complicated cloud surfaces are generated by a fractal technique applying to metaballs.

Shading models for clouds and snow are basically the same because the intensity from clouds or snow reaching the viewpoint is determined by light scattered and absorbed due to particles in clouds/snow. Even though this paper discussed a display method of clouds, the proposed method can be applied to snow.

References

[1] P. Blasi, B.L. Saec, C. Schlics, "A Rendering Algorithm for Discrete Volume Density Objects, " *Proc. of EUROGRAPHICS'93*, Vol.12, No.3 (1993) pp.201-210.

[2] J.F. Blinn, "Light Reflection Functions for Simulation of Clouds and Dusty Surfaces, " *Computer Graphics*, Vol. 16, No. 3 (1982) pp. 21-29.

[3] J.F. Blinn, "A Generalization of Algebraic Surface Drawing," *ACM Tog*, Vol.2, No.3 (1980) pp.235-256.

[4] C.F. Bohren, "Multiple scattering of light and some of its observable consequences, " *Am. J. Phys.* Vol.55, No.6 (1987) pp.524-533.

[5] M.F. Cohen, D.P. Greenberg, "The Hemicube, A Radiosity Solution for Computer Environment,", *Computer Graphics*, Vol.19, No.3 (1985) pp.31-40.

[6] W.M. Cornette, J.G. Shanks, "Physical reasonable analytic expression for the single-scattering phase function," *Applied Optics*, Vol.31, No.16 (1992) pp.3152-3160.

[7] G.Y. Gardener, "Visual Simulation of Clouds," *Computer Graphics*, Vol.19, No.3 (1985) pp.297-303.

[8] P. Hanrahan, W. Krueger, "Reflection from Layered Surfaces due to Subsurface Scattering," *Proc. of SIGGRAPH'93* (1994) pp.165-174.

[9] M. Inakage,"Volume Tracing of Atmospheric Environments," *The Visual Computer*, 7 (1991) pp.104-113.

[10] J.T. Kajiya, B.V. Herzen, "Ray tracing Volume Densities," *Computer Graphics*, Vol.18, No.3 (1984) pp.165-174.

[11] K. Kaneda, G. Yuan, E. Nakamae, T. Nishita, "Photorealistic Visual Simulation of Water Surfaces Taking into account Radiative Transfer," *Proc. of CG & CAD'91*, (China) (1991) pp.25-30.

[12] K. Kaneda, T. Okamoto, E. Nakamae, T. Nishita, "Photorealistic Image Synsesis for Outdoor scenery Under Various Atmospheric Conditions," *The Visual Computer,* Vol.7 (1991) pp.247-258.

[13] W.E. Lorensen, H.E. Cline, "Marching Cubes: a High Resolution 3D Surface Construction Algorithm," *Computer Graphics*, Vol.21, No.4 (1987) pp.163-169.

[14] R.V. Klassen, "Modeling the Effect of the Atmosphere on Light, " *ACM Transaction on Graphics*, Vol. 6, No. 3 (1987) pp. 215-237.

[15] N. Max, "Light Diffusion through Clouds and Haze," *Graphics and Image Processing*, Vol.33, No.3 (1986) pp.280-292.

[16] N. Max, "Efficient Light Propagation for Multiple Anisotropic Volume Scattering," *Proc. of the Fifth Eurographics Workshop on Rendering* (1994) pp.87-104.

[17] T. Nishita, and E. Nakamae, "Continuous tone Representation of Three-Dimensional Objects Illuminated by Sky Light," *Computer Graphics*, Vol. 20, No. 4 (1986) pp. 125-132.

[18] T. Nishita, Y. Miyawaki, E. Nakamae, "A Shading Model for Atmospheric Scattering Considering Distribution of Light Sources," *Computer Graphics*, Vol. 21, No. 4 (1987) pp. 303-310.

[19] T. Nishita, T.W. Sederberg, M. Kakimoto, "Ray Tracing Rational Trimmed Surface Patches," *Computer Graphics,* Vol.24, No.4 (1990) pp.337-345.

[20] T. Nishita, T. Shirai, K. Tadamura, E. Nakamae, "Display of The Earth Taking into Account Atmospheric Scattering, " *Proc. of SIGGRAPH'93* (1993) pp.175-182.

[21] T. Nishita, E. Nakamae, "A Method for Displaying Metaballs by using Bézier Clipping," *Proc. of EUROGRAPHICS'94*, Vol.13, No.3 (1994) c271-280.

[22] T. Nishita, E. Nakamae, "Method of Displaying Optical Effects within Water using Accumulation Buffer," *Proc. of SIGGRAPH'94* (1994) pp.373-379.

[23] H.E. Rushmeier, K.E. Torrance, "The Zonal Method for Calculating Light Intensities in The Presence of a Participating Medium," *Computer Graphics*, Vol.21, No.4 (1987) pp.293-302.

[24] G. Sakas, M. Gerth, "Sampling and Anti-Aliasing of Discrete 3-D Volume Density Textures," *Proc. of EUROGRAPHICS'91* (1991) pp.87-102.

[25] S. Sekine, "Corrected Color Temperature of Daylight(2) : Characteristics on Clear Sky and Overcast Sky," *J. Illumination Engineering Inst. Japan* , Vol.79, No.11 (1995) pp.621-627.

[26] J. Stam, E. Fiume, "Depicting Fire and Other Gaseous Phenomena Using Diffusion Processes," *Proc. of SIGGRAPH'95* (1995) pp.129-136.

Figure 7. Examples of clouds.

Figure 8. Examples of cumulonimbus.

High-resolution TIFF versions of these images can be found on the CD-ROM in:
S96PR/papers/nishita